Field-Orientation Control of a Doubly Excited Brushless Reluctance Machine

Longya Xu, *Senior Member, IEEE*, Li Zhen, *Member, IEEE*, and Eel-Hwan Kim, *Member, IEEE*

***Abstract*— In this paper, the concept and implementation of field-orientation control (FOC) of a doubly excited brushless reluctance machine (DEBRM) for variable-speed drives and generating systems are presented. A stator-flux-orientation scheme is employed to achieve decoupled control of torque and reactive power. A 2-hp DEBRM prototype system with a digital signal processor (DSP)-based controller and a bidirectional power converter is built to verify the theoretical analysis. Computer simulation and laboratory experimental results are shown in excellent agreement.**

***Index Terms*— Doubly fed motors, electric motors, field-orientation control, motor control, power electronics, reluctance motors.**

I. Introduction

THE doubly excited brushless reluctance machine (DEBRM) has gained renewed attention in recent years because of its unique structure and favorable operational characteristics with power electronics converters [3]–[8]. As shown in Fig. 1, both the primary and secondary circuits of a DEBRM are wound in the stator slots, and the reluctance rotor is essentially circuit and current free. While no rotating circuits are used, it has been proven that the secondary windings of a DEBRM emulate the functions of the rotor windings of a wound-rotor induction machine. Therefore, the equivalent circuit of the DEBRM very much resembles that of a wound-rotor induction machine, as shown in Fig. 2 [3]. It should be noted that the significance and relative magnitude of each parameter (per-unit value) of a DEBRM are quite different from those of a wound-rotor induction machine. However, the similar terminal characteristics do indicate that these two types of machines can share some common control strategies for variable-speed operations. Like a wound-rotor induction machine configured in a slip power recovery system, the DEBRM has a series of advantages, including the advantage that the inverter power rating can be substantially reduced at the sub/supersynchronous speeds near the synchronous speed. Since the DEBRM has both field and armature windings stationary and the reluctance rotor does not carry currents, the slip rings, brushes, and rotor copper losses are completely eliminated. Therefore, the system has a simpler and more reliable structure and less maintenance cost than the conventional slip power recovery system made by a wound-rotor induction machine. Besides, recent research has explored the potential of applying the DEBRM to variable-speed generating systems, such as for wind power generation. The new generating system effectively improves wind-energy-capturing capability, so that the efficiency of the overall system can be remarkably improved [3]–[5].

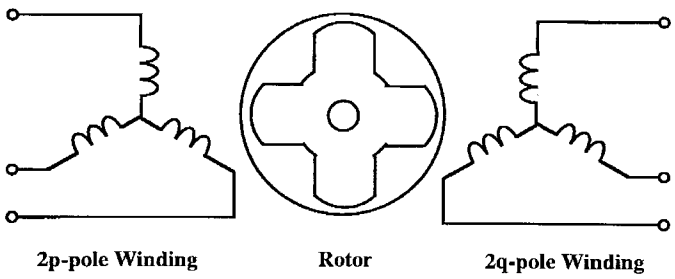

Fig. 1. Rotor and windings of a DEBRM.

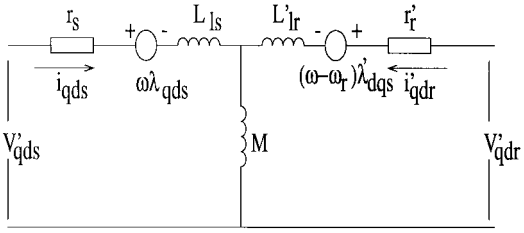

Fig. 2. Equivalent circuit of a DEBRM.

At present, scalar control methods are often used in the wound-rotor induction machine or DEBRM slip power recovery systems, in which the magnitude, frequency, and phase angle of rotor voltage and current are controlled [4], [6]. These systems are generally used in high-power, heavy-duty, and narrow-speed-range applications, where high performance is not critically important, but the rating of the power converter is a major concern. However, the slip power recovery configuration has potential for high-performance, high-efficiency, and flexible controllability if field-orientation control (FOC)

Paper IPCSD 97–65, presented at the 1996 Industry Applications Society Annual Meeting, San Diego, CA, October 6–10, and approved for publication in the IEEE TRANSACTIONS ON INDUSTRY APPLICATIONS by the Industrial Drives Committee of the IEEE Industry Applications Society. Manuscript released for publication October 20, 1997.

L. Xu is with the Department of Electrical Engineering, The Ohio State University, Columbus, OH 43210-1272 USA (e-mail: longya@ee.eng.ohio-state.edu).

L. Zhen was with the Department of Electrical Engineering, The Ohio State University, Columbus, OH 43210-1272 USA. He is now with Industrial Drives Corporation, Novato, CA 94949-5704 USA.

E.-H. Kim was with the Department of Electrical Engineering, The Ohio State University, Columbus, OH 43210-1272 USA. He is now with the Department of Electrical Engineering, College of Engineering, Cheju National University, Cheju City, Cheju-Do, 690-756 Korea.

Publisher Item Identifier S 0093-9994(98)01281-X.

is employed. Furthermore, if FOC is employed in a DEBRM generating system, it is possible to provide a convenient regulation of active and reactive power flow between the power grid and the variable-speed generator [5]–[6].

In this paper, the concept and implementation of FOC of a DEBRM for a variable-speed drive and generating system are presented. A 2-hp prototype system, with a digital signal processor (DSP) controller and a bidirectional power converter, is built to experimentally investigate the characteristics of the DEBRM slip power recovery sytem and to verify theoretical analysis. Extensive simulation and experimental results are presented to support the discussion.

II. Field-Orientation Control of DEBRM

To illustrate the concept of FOC, the system connection and the waveforms of the primary (armature) and secondary (field) MMF's, field flux, and rotor saliency of a DEBRM are drawn in Fig. 3. The DEBRM machine is connected in the slip power recovery configuration and has dual (two-pole primary and six-pole secondary) windings on the stator and a four-pole salient reluctance rotor. As shown in Fig. 3(b), two rotating MMF's are produced when two sets of three-phase currents flow through the dual stator windings of two-pole and six-pole numbers. A two-pole flux is generated along the airgap, due to the modulation provided by the four-pole salient reluctance rotor over the six-pole MMF. It is this two-pole flux, resulting from modulation, that interacts with the two-pole MMF to generate the electromagnetic torque. It is seen that, if the two-pole flux resulting from modulation and the two-pole MMF due to the regulated currents are orthogonal in the airgap space, maximum torque production is achieved. Under such a condition, the DEBRM is in the field-oriented operation mode. Given such a concept of FOC of a DEBRM, the major topic of this paper is how FOC can be realized and what operational characteristics are expected.

As stated earlier, because of the modulation provided by the salient reluctance rotor over the MMF's, the operation principle of a DEBRM is very similar to that of a wound-rotor induction machine [1]. Therefore, DEBRM can be expressed by differential equations of the same form as those for the wound-rotor induction machine. Note that, in terms of FOC, the DEBRM under discussion can be expressed as either a six-pole or a two-pole machine, depending on the selection of transformation. In this case, we describe FOC of the DEBRM as a two-pole machine electrically. The dynamic equations of a DEBRM in the arbitrary rotating d-q reference frame are [1]

$$v_{d1} = r_1 i_{d1} + \frac{d\lambda_{d1}}{dt} - \omega\lambda_{q1} \tag{1}$$

$$v_{q1} = r_1 i_{q1} + \frac{d\lambda_{q1}}{dt} + \omega\lambda_{d1} \tag{2}$$

$$v_{d2} = r_2 i_{d2} + \frac{d\lambda_{d2}}{dt} - (\omega - \omega_r)\lambda_{q2} \tag{3}$$

$$v_{q2} = r_2 i_{q2} + \frac{d\lambda_{q2}}{dt} + (\omega - \omega_r)\lambda_{d2} \tag{4}$$

$$\lambda_{d1} = L_1 i_{d1} + L_m i_{d2} \tag{5}$$

$$\lambda_{q1} = L_1 i_{q1} + L_m i_{q2} \tag{6}$$

$$\lambda_{d2} = L_m i_{d1} + L_2 i_{d2} \tag{7}$$

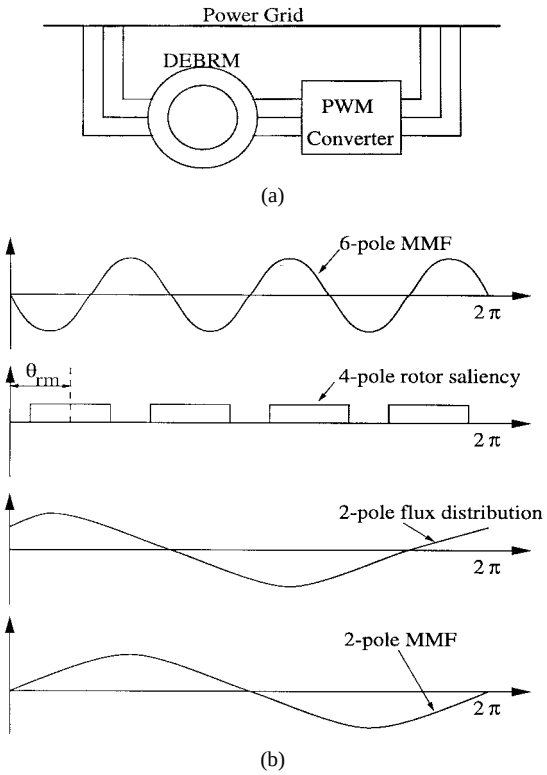

Fig. 3. FOC of a DEBRM. (a) Connection of slip power recovery system. (b) MMF modulation in a DEBRM.

$$\lambda_{q2} = L_m i_{q1} + L_2 i_{q2} \tag{8}$$

$$T_e = \frac{3}{2}\frac{P}{2}\frac{L_m}{L_1}(\lambda_{q1} i_{d2} - \lambda_{d1} i_{q2}) \tag{9}$$

$$T_e = J\frac{2}{P}\frac{d\omega_r}{dt} + B\frac{2}{P}\omega_r + T_L \tag{10}$$

where $P = 2(p_1 + p_2)$ (p_1 and p_2 are the pole pair number of the two stator windings, respectively). ω_1, ω_2, and ω_r are the electrical angular frequencies in the first winding, the secondary winding, and the rotor speed, respectively. J and B are the rotor inertia and friction. The subscripts "1" and "2" refer to the quantities associated with the primary and the secondary windings.

Field orientation along the primary winding field flux λ_{dq1} can be realized by selecting the primary winding flux as the reference frame and locking the d axis to λ_{dq1}. Then, $\lambda_{q1} \equiv 0$. Hence, the following important relations hold:

$$v_{d1} = r_1 i_{d1} + \frac{d\lambda_{d1}}{dt} \tag{11}$$

$$v_{q1} = r_1 i_{q1} + \omega_1\lambda_{d1} \tag{12}$$

$$\lambda_{d1} = L_1 i_{d1} + L_m i_{d2} \tag{13}$$

$$0 = L_1 i_{q1} + L_m i_{q2} \tag{14}$$

$$T_e = -\frac{3}{2}\frac{P}{2}\frac{L_m}{L_1}\lambda_{d1} i_{q2}. \tag{15}$$

Recall that, in the DEBRM configuration, the primary windings are always connected to a utility power supply, as shown in Fig. 3(a). Hence, the level of the primary winding flux remains approximately unchanged, constrained only by the magnitude and frequency of the line voltage of the power

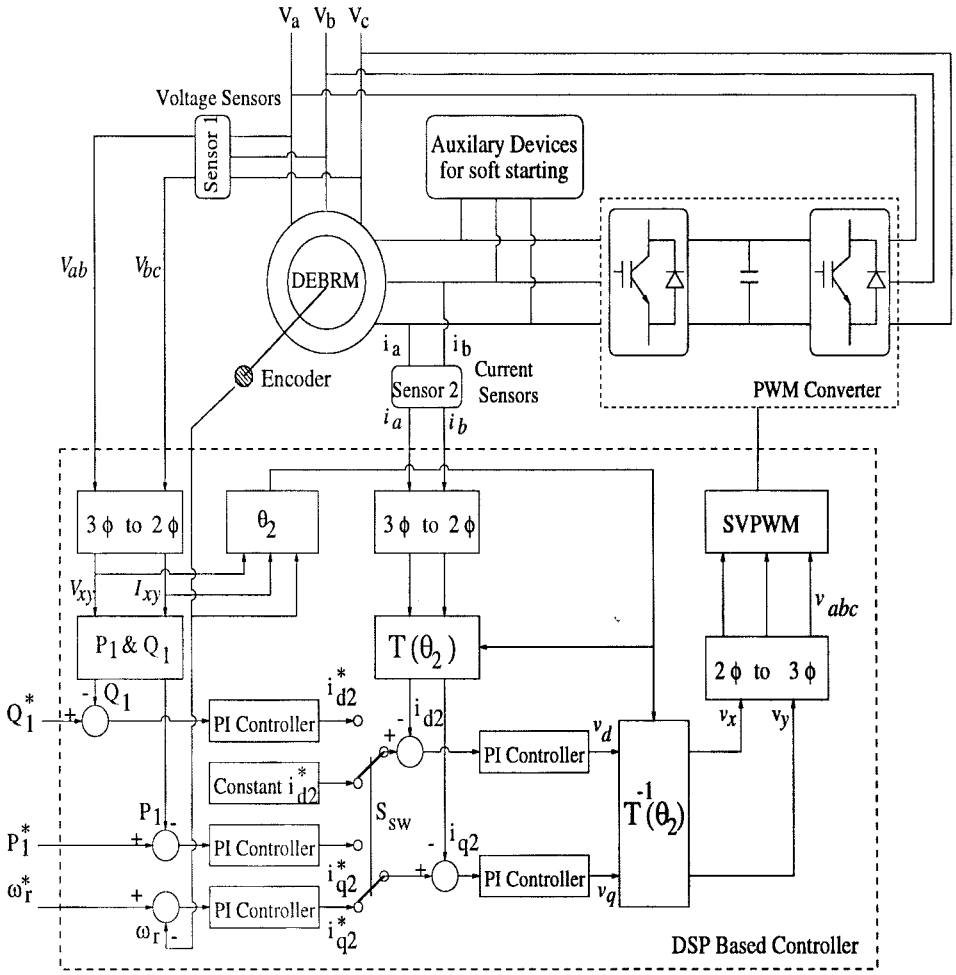

Fig. 4. Configuration of the FOC of a DEBRM.

system. The statement of almost constant flux can be derived from (12) if the voltage drop of winding resistance is neglected [5]. Therefore, as seen from the torque equation, the instantaneous torque control is achievable by controlling the secondary winding quadrature current component i_{q2}.

In addition, active and reactive power at the terminal of the primary winding can be derived as

$$P_1 = -\frac{3}{2}\frac{L_m}{L_1}\omega_1\lambda_{d1}i_{q2} \tag{16}$$

$$\begin{aligned} Q_1 &= \frac{3}{2}(v_{q1}i_{d1} - v_{d1}i_{q1}) \\ &= \frac{3}{2}\omega_1\lambda_{d1}i_{d1} \\ &= \frac{3}{2}\frac{1}{L_1}\omega_1\lambda_{d1}(\lambda_{d1} - L_m i_{d2}). \end{aligned} \tag{17}$$

Note that the fact that $\lambda_{d1} = \textit{constant}$ and $r_1 \doteq 0$ is used in deriving the equation for Q_1.

Therefore, once the machine works in the generator mode, active power control can be realized by controlling the quadrature component in the secondary winding current i_{q2} according to (16), and the reactive power can be regulated by controlling the secondary winding current direct component i_{d2} according to (17). Notice that, in the slip power control scheme, flux control is not achievable, since the flux is clamped by the strong power system to a constant level, but control of reactive power is possible.

III. Implementation of FOC

Based on the principle discussed in Section II, two control loops are constructed to realize the torque (active power) control and reactive power control, as shown in Fig. 4. The FOC is accomplished, along with the inner current regulation loop. The variable-speed control or active/reactive power control is realized by the outer speed controller or active/reactive controller.

A. FOC Through Secondary Current

Correct FOC requires that the d axis of the reference frame is locked to the primary winding flux and i_{d2} and i_{q2} are controlled to be parallel and orthogonal to λ_{d1}. As derived in [1], the primary frequency ω_1, the secondary frequency ω_2, and the rotor mechanic speed $\omega_{\rm rm}$ satisfy the following constraint (for the case where the abc sequence of the three phase currents in the two sets of windings are the same):

$$\omega_1 - \omega_2 = (p_1 + p_2)\omega_{\rm rm}. \tag{18}$$

Hence,

$$\theta_2 = \theta_1 - (p_1 + p_2)\theta_{\rm rm}. \tag{19}$$

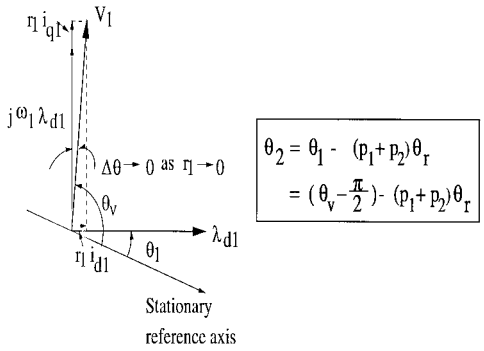

Fig. 5. θ_2 estimation.

A space vector diagram is shown in Fig. 5 to illustrate the relationship between angle θ_V and θ_1. Note that the angle θ_1 is the primary flux angle. Since r_1 is usually very small, $r_1 i_{q1}$ and $r_1 i_{d1}$ can be neglected, and θ_1 can be simply replaced by $\theta_V - \frac{\pi}{2}$, as shown in Fig. 5, where θ_V is the phase angle of the primary winding voltage. Therefore, by measuring the rotor angle $(p_1 + p_2)\theta_{\rm rm}$ and the primary voltage angle θ_V, the secondary current angle θ_2 can be determined.

B. Soft Starting and Speed Control

Since the rated power of the inverter is reduced to half of the machine's rated value, it is very important to limit the starting current of the machine below the rated value of the inverter. In our implementation, the machine is started in the following three steps.

- The machine is freely accelerated close to the synchronous speed (with secondary resistance).
- The inverter is switched into the secondary windings with top or bottom power switches on.
- Speed control is applied to bring the machine to the desired (below or above synchronous) speed.

In this way, not only is the inverter overcurrent avoided, but the inrush current in the machine is also eliminated.

Once the rotor speed is close to the synchronous speed, the switch $S_{\rm sw}$ (software implementation) will be switched to the lower position, as indicated in Fig. 4, by which the speed control loop is activated. Constant flux control can be obtained by setting the flux command current i_{d2}^* to a constant. The torque command current i_{q2}^* is generated by a proportional integral (PI) controller, based on the speed error. Note that the current limiter is included in the PI controller to avoid overcurrent.

Fig. 6 shows the computer simulation result of DEBRM FOC. In the figure, $\omega_{\rm ref}$, $\omega_{\rm rm}$, i_{q2}, and i_{a2} express the speed command, the actual speed, the command current in the secondary winding, and the phase current in the secondary windings, respectively.

First, the machine is freely accelerated to synchronous speed (900 r/min). Then, the power inverter is switched into the secondary windings of the machine, and the speed control loop is connected to drive the machine to supersynchronous speed (1000 r/min) at $t = 2.2$ s and, then, undersynchronous speed

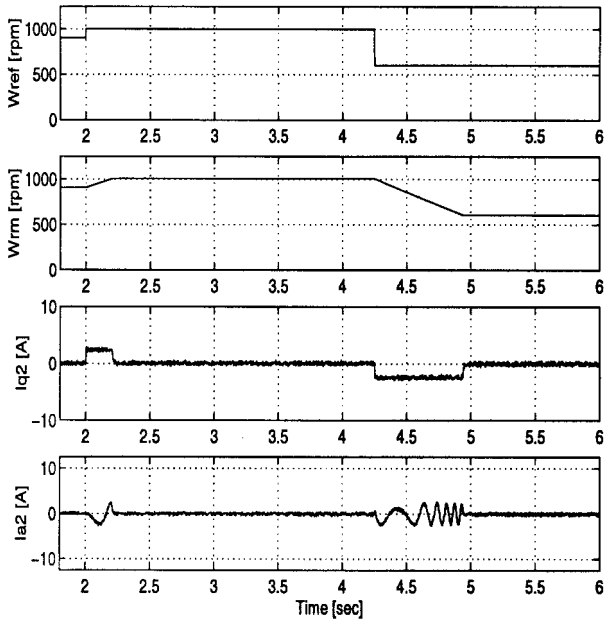

Fig. 6. Computer simulation of DEBRM step speed response.

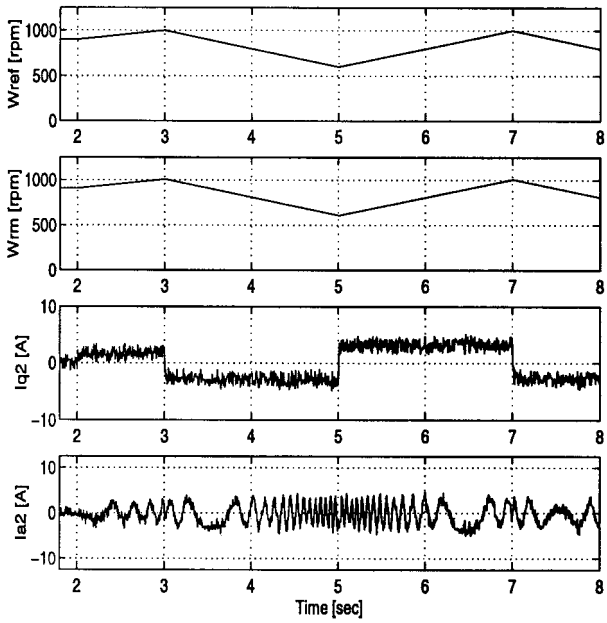

Fig. 7. Computer simulation of DEBRM variable speed tracking.

(600 r/min) at $t = 4.9$ s. No inrush current is generated when the inverter is switched into the secondary windings.

Fig. 7 is the DEBRM speed tracking performance based on FOC. After the machine is accelerated to the synchronous speed (900 r/min), a triangular speed around synchronous speed (between 600 and 1000 r/min) is commanded. Under the FOC, the actual speed of the machine overlaps the command speed, showing a perfect speed tracking.

C. Active/Reactive Power Control

As mentioned before, when DEBRM operates as a generator, active/reactive power control is meaningful and can be

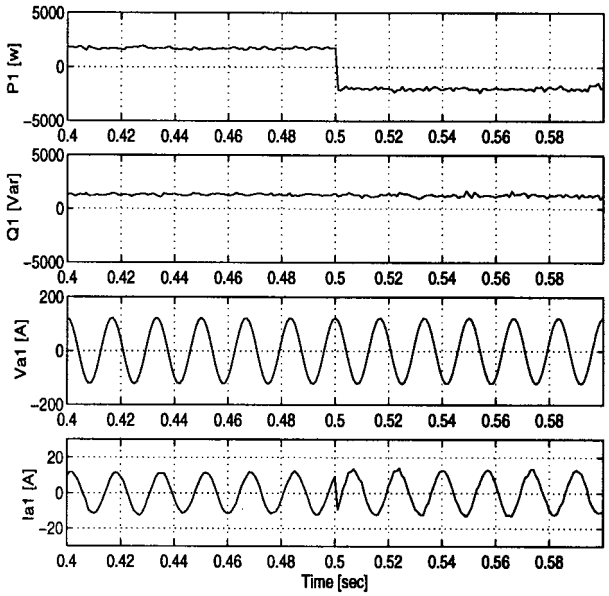

Fig. 8. Computer simulation of DEBRM decoupled active power control.

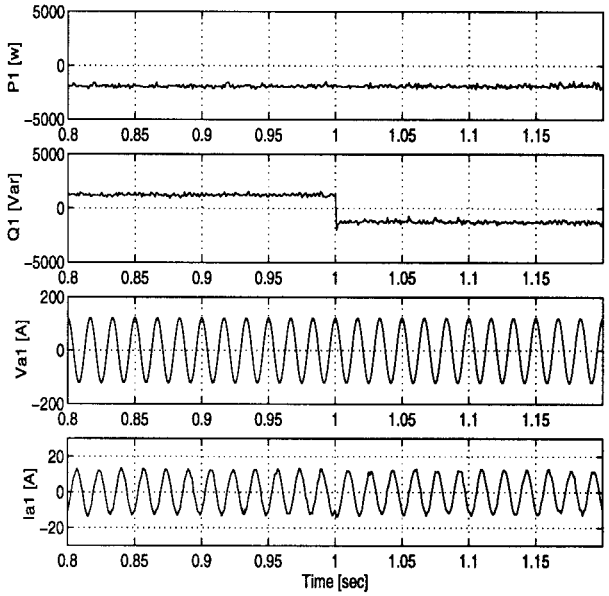

Fig. 9. Computer simulation of DEBRM decoupled reactive power control.

accomplished by controlling i_{q2} and i_{d2}, as seen in (16) and (17). Strictly speaking, two voltage sensors and four current sensors (two voltage sensors and two current sensors in the primary winding and the other two current sensors in the secondary winding), are required to implement the active/reactive power control. However, the DEBRM generating system is designed to operate very close to the synchronous speed, so that the $\omega_1\lambda_{d1} \gg r_1 i_{q1}$ in (12). Therefore, the flux in the first winding λ_{d1} can be simply expressed by

$$\lambda_{d1} = \frac{v_{q1}}{\omega_1} \tag{20}$$

indicating that the two current sensors in the primary winding are not needed, and the active and reactive power can be calculated by the following equations:

$$P_1 = -\frac{3}{2}\frac{L_m}{L_1} v_{q1} i_{q2} \tag{21}$$

$$Q_1 = \frac{3}{2}\frac{1}{L_1} v_{q1}\left(\frac{v_{q1}}{\omega_1} - L_m i_{d2}\right). \tag{22}$$

In order to implement active/reactive power control, $S_{\rm sw}$ initially activates the speed control loop, and the machine is accelerated to the required speed. Then, $S_{\rm sw}$ is changed to activate power control (the top branch), as shown in Fig. 4, for active/reactive power control.

The simulation result of active/reactive power control is shown in Figs. 8 and 9. Unity power factor control is obtained by FOC. The phase angle change of the current is also illustrated when the machine operation mode is changed from motoring to generating mode.

IV. Experimental Results

The FOC of a DEBRM is implemented in the Power Electronics and Electric Machines Laboratory at The Ohio State University. The experimental setup is constructed according to the slip power recovery scheme. A 2-hp prototype of a DEBRM with $P = 2(p_1 + p_2) = 8$ is used. A bidirectional power flow converter with half of the machine power rating is connected to the secondary winding. Control algorithms are accomplished by a Motorola DSP56001-based controller, as shown in Fig. 4. The specifications and parameters of the DEBRM are as follows:

$L_{l1} = 12.1$ mH, $V_1 = 220$ V, $I_1 = 4.5$ A
$L_{l2} = 11$ mH, $R_1 = 0.4\ \Omega$, $R_2 = 0.32\ \Omega$
$L_m = 30$ mH, $P = 2$ hp, $n = 900$ r/min.

A. Variable-Speed Control

The experimental results of the DEBRM variable-speed drive are presented in Figs. 10 and 11, which show the step speed response and speed tracking, respectively. Initially, the machine is accelerated and operates at the synchronous speed (900 r/min). Then, a step speed command and a triangular speed command (range from 600 to 1000 r/min) are applied separately, covering super and subsynchronous speed range. As seen from the figure, the machine can respond and track the command speeds very satisfactorily under the correct FOC.

Fig. 11 shows the variable-speed tracking performance of the DEBRM with FOC. A triangular speed command (range from 600 to 1000 r/min) is applied, covering both super and subsynchronous speed range. As seen in the figure, the machine can track the command speed very satisfactorily. In both experiments, no inrush current occurs when the inverter is switched into the secondary winding.

B. Generator/Motor Operation

The DEBRM, similar to a wound-rotor induction machine, can conveniently operate in a generating or motoring mode at sub and supersynchronous speeds. The capability of operating in a generating or motoring mode at both subsynchronous and supersynchronous speeds is a distinguishing feature of the DEBRM, as opposed to a singly fed cage machine, where only subsynchronous speed motoring and supersynchronous speed generating modes are possible. Fig. 12 shows the experimental

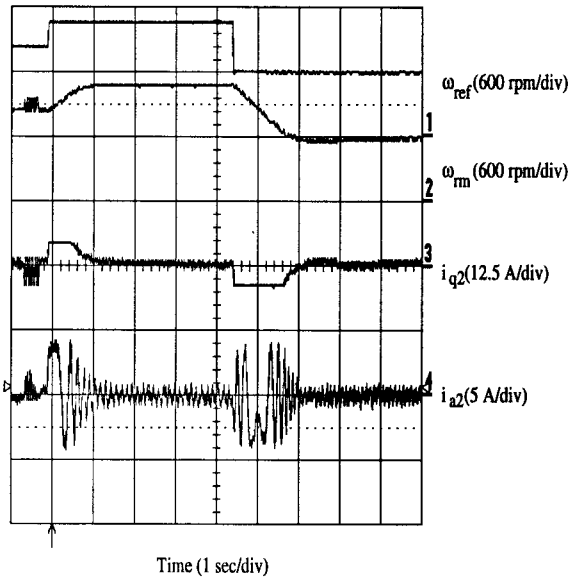

Fig. 10. Experimental result of DEBRM step speed response.

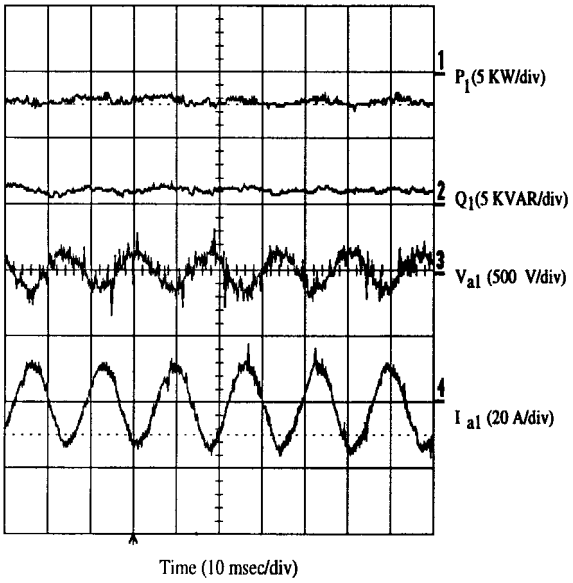

Fig. 12. Experimental result of DEBRM in generating operation.

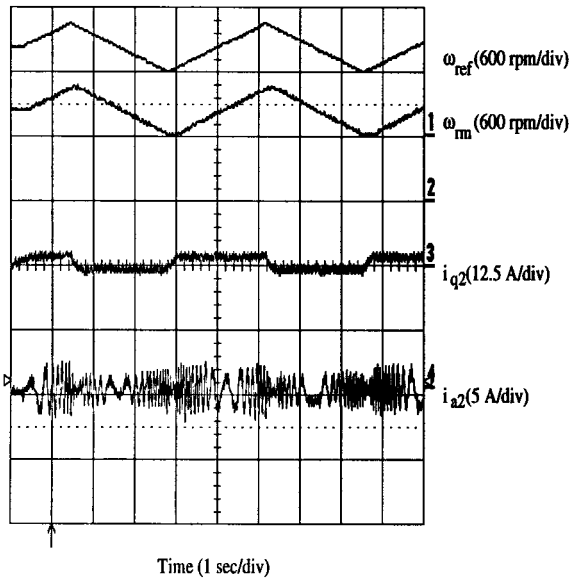

Fig. 11. Experimental result of DEBRM variable-speed tracking.

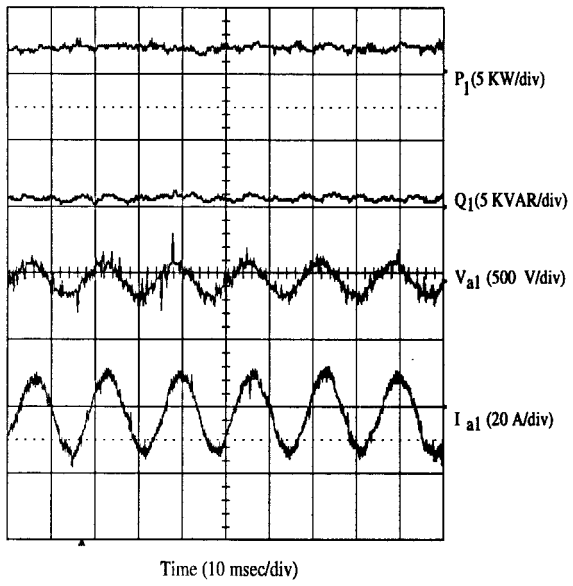

Fig. 13. Experimental result of DEBRM in motoring operation.

results of the DEBRM in generating mode at a subsynchronous speed (600 r/min) and Fig. 13 shows the motoring mode at a supersynchronous speed (1000 r/min). In Fig. 12, the phase current of the primary winding lags the phase voltage by an angle greater than 90°, indicating that the primary active power P_1 is negative and the DEBRM is in the generating mode. On the other hand, in Fig. 13, the current lags the voltage by an angle less than 90°, indicating a motoring mode (P_1 is positive). In these experiments, no reactive power control is applied and the DEBRM draws reactive power from the power grid to maintain the magnetizing requirement.

C. Decoupled Active/Reactive Power Control

Decoupled control of active power and reactive power in a DEBRM is illustrated in this section, where the DEBRM operates at a subsynchronous speed (600 r/min). Fig. 14 shows the experimental results of active power control where the DEBRM is changed from generating mode to motoring mode within 0.5 s. (P_1 changing from negative to positive). As seen in the figure, the primary reactive power Q_1 is not affected at all when the transition of active power occurs.

The experimental result of decoupled reactive power control is shown in Fig. 15, where the DEBRM operates in the generating mode with a lagging power factor at subsynchronous speed (600 r/min). At $t = 1.75$ s, a step reactive power change is commanded to change the power factor from lagging to leading state. As seen in the figure, the active power keeps constant. The results shown in Figs. 14 and 15 indicate that decoupled active and reactive power control has been effectively achieved.

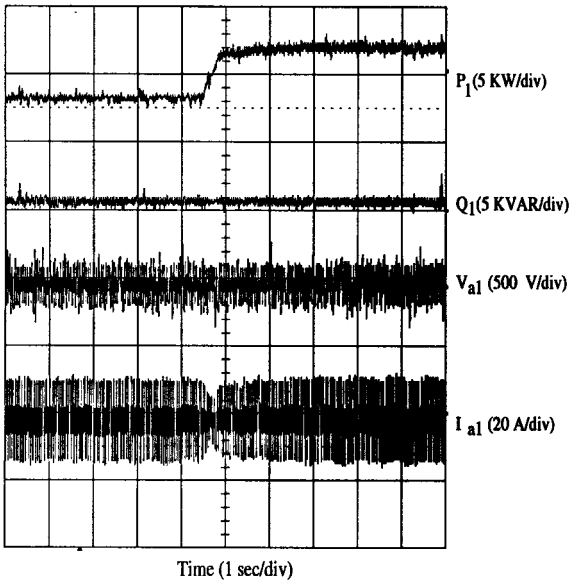

Fig. 14. Experimental result of DEBRM decoupled active power control (from generating to motoring).

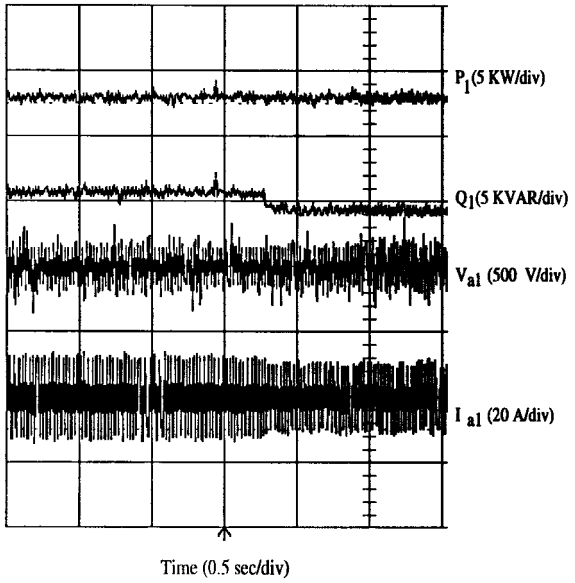

Fig. 15. Experimental result of DEBRM reactive power control.

V. Conclusion

The concept and implementation of DEBRM FOC have been discussed in this paper. Stator-flux orientation is employed to achieve decoupled control of torque and active/reactive power through the secondary currents. Thus, variable-speed drive and generator operation with decoupled active/reactive power control can be achieved by the DEBRM systems. Computer simulation and extensive experimental results have shown the effectiveness of the DEBRM control scheme.

References

[1] F. Liang, L. Xu, and T. A. Lipo, "*D-Q* analysis of a variable speed doubly AC excited reluctance motor," *Elect. Mach. Power Syst.*, vol. 19, no. 2, pp. 125–138, Mar. 1991.

[2] T. A. Lipo, "Variable speed generator technology options for wind turbine generators," presented at the DOE/NASA Workshop Horizontal-Axis Wind Turbine Technology, Cleveland, OH, May 1984.

[3] E. Akpinar and P. Pillay, "Modeling and performance of slip energy recovery induction motor drives," *IEEE Trans. Energy Conversion*, vol. 5, pp. 203–210, Mar. 1990.

[4] L. Xu and Y. Tang, "High efficient wind power generation by the doubly excited brushless reluctance machine," presented at the American Wind Power Energy Association WindPower'93 Conf., San Francisco, CA, July 1993.

[5] L. Xu and Y. Tang, "A novel wind power generating system using field orientation controlled doubly-excited brushless reluctance machine," presented at the IEEE-IAS Annu. Meeting, Houston, TX, Oct. 1992.

[6] C. Brune, R. Spee, and A. K. Wallace, "Experimental evaluation of a variable-speed double-fed wind-power generating system," presented at the IEEE-IAS Annu. Meeting, Toronto, Ont., Canada, Oct. 1993.

[7] G. A. Smith, "A current-source inverter in the secondary circuit of a wound rotor induction machine motor provides sub- and super-synchronous operation," *IEEE Trans. Ind. Applicat.*, vol. IA-17, pp. 399–406, July/Aug. 1981.

[8] M. G. Ioannides and J. A. Tegopoulos, "Performance of a double-fed induction machine motor with controlled rotor voltage and phase angle," *IEEE Trans. Energy Conversion*, vol. EC-2, pp. 301–307, June 1987.

[9] Y. Liao and C. Sun, "A low cost, robust position sensorless control scheme for DFRM drive," in *Proc. IEEE-IAS Annu. Meeting*, 1993, pp. 437–444.

[10] D. Zou, R. Spee, and G. Alexander, "Experimental evaluation of a rorot flux oriented control clgorithm for brushless doubly-fed machines," in *Conf. Rec. IEEE-PESC Conf.*, 1996, pp. 913–919.

Longya Xu (S'89–M'90–SM'93) received the M.S. and Ph.D. degrees in electrical engineering from the University of Wisconsin, Madison, in 1986 and 1990, respectively.

He has served as a Consultant to numerous companies, including Raytheon Company, U.S. Wind Power Company, General Motors, Ford, and Unique Mobility Inc. In 1990, he joined the Department of Electrical Engineering, The Ohio State University, Columbus, where he is currently an Associate Professor. His research and teaching interests include dynamic modeling and optimized design of electrical machines and power converters for variable-speed generating and drive systems.

Dr. Xu currently serves as the Secretary of the Electric Machines Committee of the IEEE Industry Applications Society (IAS) and is an Associate Editor of the IEEE Transactions on Power Electronics. He received the 1990 First Prize Paper Award from the IAS Industrial Drives Committee. In 1991, he won a Research Initiation Award from the National Science Foundation. He is also the recipient of the 1995 Lumley Research Award from the College of Engineering, The Ohio State University, for his outstanding research accomplishments.

Li Zhen (S'95–M'96) received the B.S.E.E. and M.S.E.E. degrees from Shanghai Jiao Tong University, Shanghai, China, in 1982 and 1985, respectively, and the Ph.D. degree from The Ohio State University, Columbus, in 1996.

From 1985 to 1988, he was an Application Engineer with the Central China Electric Power Administration, where he was engaged in computer applications in power system analysis and real-time control. In 1988, he was a Lecturer at Shanghai Jiao Tong University, where he taught and conducted research in the area of power system protection and control. From 1993 to 1996, he was a Graduate Research Associate in the Electric Machines and Power Electronics Group, Department of Electrical Engineering, The Ohio State University. He is currently with Industrial Devices Corporation, Novato, CA, working on research and design in the area of industrial servo control. His research interests include DSP-based servo control systems, power electronics, and high-performance servo drives.

Eel-Hwan Kim (S'89–M'91) was born in Korea in 1962. He received the B.S., M.S., and Ph.D. degrees in electrical engineering from Chung Ang University, Korea, in 1985, 1987, and 1991, respectively.

Since 1991, he has been with the Department of Electrical Engineering, Cheju National University, Cheju City, Korea. From 1995 to 1996, he was with the Department of Electrical Engineering, The Ohio State University, Columbus, as a Visiting Scholar. His research interests include the modeling and control of electric machine systems using power electronics.